Final Report
on
Contract No. N00014-86-C-0570

ULF/VLF Ocean Bottom Seismo-Acoustics

Submitted to the
Office of Naval Research

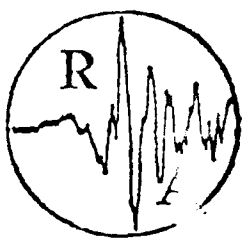

Rondout Associates, Incorporated
P.O. Box 224
Stone Ridge, NY 12484
(914) 687-9150

February 27, 1990

Introduction

The original research under this contract was directed toward comparison of ocean bottom seismometer and hydrophone data with ocean sub-bottom seismometer data and with appropriate synthetics to determine the effect of sub-bottom structure on the signals received; expected propagation loss; predominant modes of propagation; instrument signal distortion and excess noise; expected spacial coherence; and expected improvement from polarization and array processing. During the first and subsequent years of the contract, research emphasis was re-directed toward analysis and interpretation of data from the Columbia-Point Arena ocean bottom seismic station (OBSS) emphasizing the objectives of the ONR Accelerated Research Initiative in ULF/VLF Ocean Seismo-Acoustics.

The most extensive existing set of ocean bottom data on ULF/VLF seismic background noise and signals was obtained from OBSS, which operated for over six years (1966-1972) about 200 km west of San Francisco at a depth of 3900 m. The OBSS included a Lamont long-period (LP) triaxial seismometer (15 sec natural period, originally developed for lunar use); three-component short-period (SP) system (1 sec natural period); long-period (crystal) hydrophone; short-period (coil-magnet) hydrophone; ultralong-period (Vibratron) pressure transducer; thermometer; current amplitude sensor; and a current direction sensor. It was connected to shore via cable and LP and SP components were recorded separately on FM tape as well as on seismograph drum recorders. During this research, original FM tapes from the OBSS long- and short-period (LP/SP) hydrophones and LP and SP three-component seismometers were digitized to obtain ULF/VLF spectra and covariances during quiet and noisy times and during passage of vessels and earthquake wavetrains. These were compared with available source information on sea/swell condition, tidal currents, earthquakes, and shipping. Analyses were conducted in the frequency band .002 to 5 Hz.

Coherent energy peaks near 0.14, and 0.06 Hz suggest fundamental mode Rayleigh wave motion propagating shoreward. Coherent energy near .30 Hz appears to be variable. Pressure variations near 0.01 Hz and lower frequency correlate with wave heights along the California coast and appear to produce forced deformation of the bottom. Two intense NE Pacific storms with hurricane force winds occurred during one two week time period. Time variations of spectra and of amplitude and phase coherencies of the four-component OBSS data were related to the storm histories and to local weather/wave conditions and used to identify motion (seismic wave) types and directions of propagation.

The research supported by this contract is summarized in the reports and publications listed below. A reprint and a preprint of two publications are included as appendices A - "Particle Motion and Pressure Relationships of Ocean Bottom Noise: 3900 m Depth; 0.003 to 5 Hz" and B - "Ocean-Bottom ULF Seismo-Acoustic Noise: .002 to .4 Hz."

Reports and Publications Resulting From This Research

Barstow, N., G. H. Sutton, and J. A. Carter, "Particle motion and pressure relationships of ocean bottom noise: 3900 m depth, 0.003 to 5 Hz," *Geophys. Res. Let.*, vol. 16, pp. 1185-1188, 1989.

Carter, J. A., G. H. Sutton, A. Suteau-Henson, and F. K. Duennebier, "Analysis of Ocean-Subbottom Seismograph (OSS) data," *Proceeding of Ocean Seismo-Acoustics Symposium, NATO ASI series*, pp. 553-564, Plenum Press, 1986.

Sutton, G. H., "Ocean bottom seismology: history and current status," *Ocean Seismo-acoustics*, pp. 821-840, T. Akal and J. M. Berkson, ed., Plenum Press, 1986.

Sutton, G. H., J. A. Carter, and N. Barstow, "Ambient ULF/VLF ocean-bottom noise 200 km west of San Francisco: motion and pressure 0.002 - 20 Hz," *J. Acoust. Soc. Am.*, vol. 82, sup. 1, p. S63, 1987.

Sutton, G. H. and F. K. Duennebier, "Optimum design of ocean bottom seismometers," *Marine Geophys. Res.*, vol. 9, pp. 47-65, 1987.

Sutton, G. H., N. Barstow, and J. A. Carter, "Long-period seismic measurements on the ocean floor," *Proceedings of a Workshop on Broad-band Downhole Seismometers in the Deep Ocean*, pp. 126-141, G. M. Purdy and A. M. Dziewonski, ed., Woods Hole Oceanographic Institution, 1988.

Sutton, G. H., N. Barstow, and J. A. Carter, "Particle motion and pressure relationships of ocean bottom noise at 3900 m depth: 0.003 to 5 Hz," *Proceedings of a Workshop on ULF/VLF (0.001 to 50 Hz) Seismo-Acoustic Noise in the Ocean*, pp. A32-A39, G. H. Sutton, ed., Institute for Geophysics, Univeristy of Texas, Austin, 1988.

Sutton, G. H., N. Barstow, and J. A. Carter, "Particle motion and pressure relationships of ocean bottom noise at 3900 m depth: 0.001 to 10 Hz," *Seism. Res. Let.*, vol. 59, p. 48, 1988.

Sutton, G. H. and F. K. Duennebier, "Avoiding signal distortion and excess noise in OBS," *Workshop on Exploration of Deep Continental Margin Crust with Closely Spaced Shots and Receivers at Houston Area Research Center (HARC)*, Co-Covenors: M. Talwani, P. L. Stoffa and W. D. Mooney, The Woodlands, Texas, 1989.

Sutton, G. H., N. Barstow, and J. A. Carter, "Ocean-bottom seismo-acoustic ambient noise: .004 to .4 Hz," *Transactions, Am. Geophys. Union*, vol. 70, p. 1154, 1989.

Sutton, G. H. and N. Barstow, "Ocean-bottom ULF seismo-acoustic ambient noise: .002 to .4 Hz," *J. Acoust. Soc. Am.*, in press, 1990.

GEOPHYSICAL RESEARCH LETTERS, VOL. 16, NO. 10, PAGES 1185-1188, OCTOBER 1989

PARTICLE MOTION AND PRESSURE RELATIONSHIPS OF OCEAN BOTTOM NOISE: 3900 M DEPTH; 0.003 to 5 HZ

Noël Barstow, George H. Sutton, and Jerry A. Carter

Rondout Associates, Incorporated

Abstract. Samples of ocean bottom noise in the frequency band 0.003 to 5 Hz are analyzed for coherency and amplitude and phase relationships among pressure and the three components of particle motion. Data available from the Columbia-Point Arena ocean bottom seismic station (38° 09.2′N, 124° 54.4′W) provide examples of different noise conditions. Coherent energy peaks near 0.14, and 0.06 Hz suggest fundamental mode Rayleigh wave motion propagating shoreward. Coherent energy near .30 Hz appears to be variable. Pressure variations near 0.01 Hz and lower frequency correlate with wave heights along the California coast and appear to produce forced deformation of the bottom.

Introduction

Possibly the most extensive set of ocean bottom data on long period seismic background noise and signals was obtained from the Columbia-Point Arena Ocean Bottom Seismic Station (OBSS). OBSS operated for over six years and a number of papers [e.g., Auld et al., 1969; Latham and Nowroozi, 1968; Piermattei and Nowroozi, 1969; Sutton et al., 1965; Nowroozi et al., 1968 and 1969] have been published using OBSS data on, e.g., gravity and pressure tides and tidal currents; ocean bottom microseisms; Rayleigh waves from pure oceanic paths and across the continental margin; and local and regional earthquakes.

The Columbia-Point Arena OBSS was installed on 18 May, 1966 at 38° 09.2′N, 124° 54.4′W about 200 km west of San Francisco at a depth of 3903 meters. It was in continuous operation for more than six years, until 11 September 1972. The OBSS included a Lamont long-period (LP) triaxial seismometer (15 sec natural period, originally developed for lunar use); three-component short-period (SP) system (1 sec natural period); long-period (crystal) hydrophone; short-period (coil-magnet) hydrophone; ultralong-period (Vibratron) pressure transducer; thermometer; current amplitude sensor; and a current direction sensor.

Data

The data, recorded on two 7-channel instrumentation-quality FM tape recorders and on seismograph-type drum recorders and strip chart recorders, are currently stored at Lamont-Doherty Geological Observatory. Short- and long-period response curves are published in Sutton et al. [1965]. The long-period data are digitized at 8 sps and the short-period data at 80 sps; a four-pole Bessel anti-alias filter was applied at a frequency equal to one-fifth the sample rate. For each sample of signal or noise digitized, we also digitized seismometer calibration pulses for that date. After system responses are removed from simultaneous noise samples of long- and short-period data, for each of the three components of ground motion, the LP and SP noise spectra are very well matched between about 0.1 and 0.5 Hz (system noise limits the spectra above 0.5 Hz for LP data and below 0.1 Hz for SP data).

To further check the accuracy of the data, we digitized a few earthquakes to verify polarities for all eight components, to compare m_b magnitude determinations with those published, and to compare pressure-vertical relationships with theoretical values. The only potential problem we encountered was with the pressure data. Unlike the seismometers, the hydrophone channels have no daily calibration pulses. Comparison of observed and theoretical P/Z amplitude and phase relationships for digitized earthquake P-waves and Rayleigh waves has convinced us that the 6 dB/octave high-pass corner at 3 Hz, included in the original calibration curve for the coil (SP) hydrophone, does not exist and should be replaced with a 0.3 Hz, 6dB/octave high-pass corner. The original 3 Hz corner represents the effect of an hydraulic relief

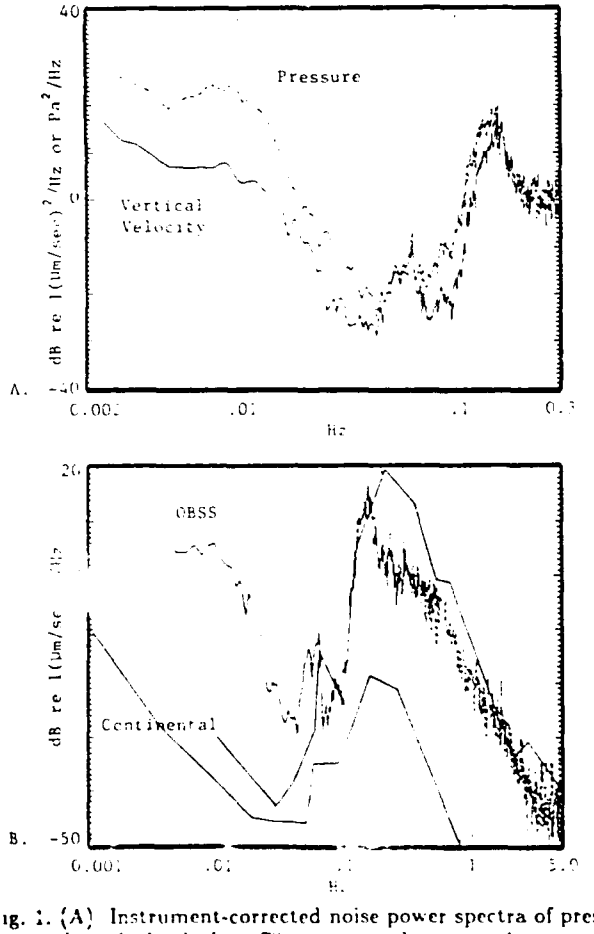

Fig. 1. (A) Instrument-corrected noise power spectra of pressure and vertical velocity. The pressure data may be up to 6 dB too low. (B) Vertical velocity power spectra for OBSS compared with spectra for continental stations under quiet and noisy conditions (Jon Peterson, USGS, unpublished data). The OBSS data are simultaneous samples from LP (solid line) and SP (dashed line) seismometers.

Paper number 89GL01618.
0094-8276/89/89GL-01618$03.00

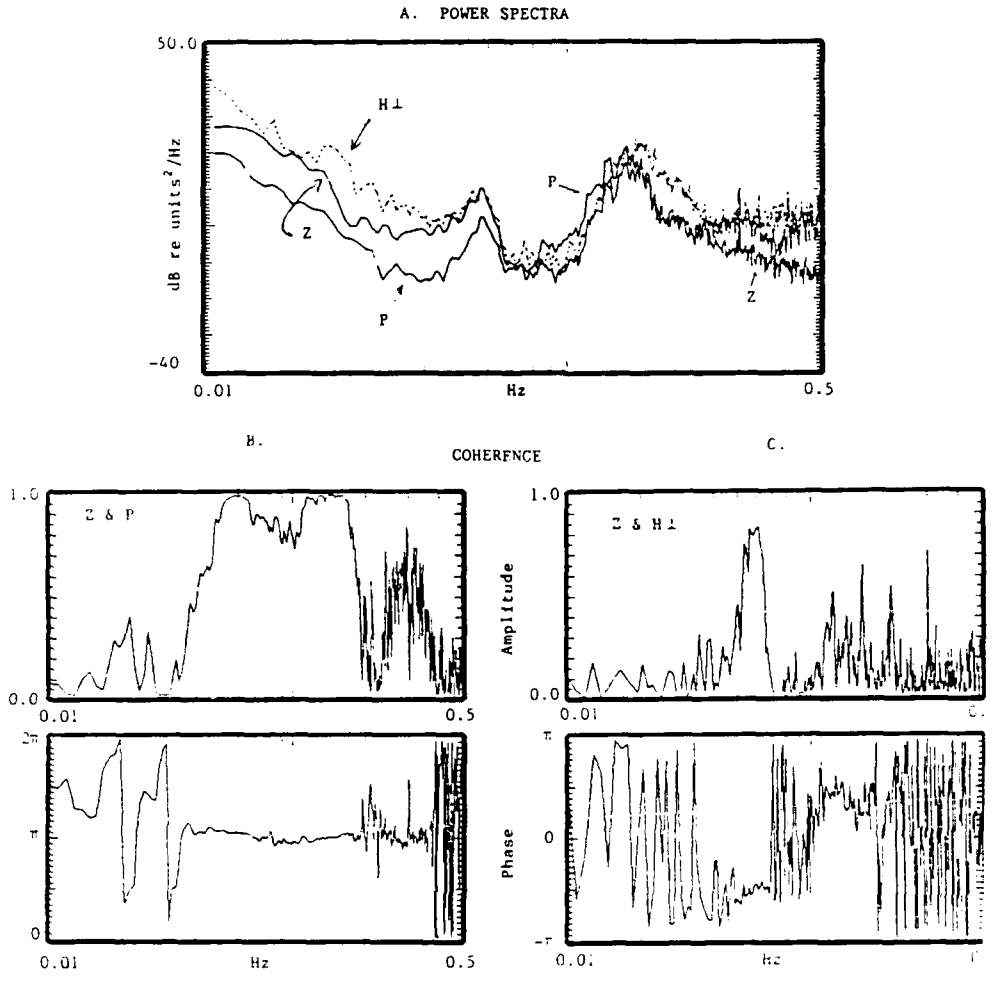

Fig. 2. (A) Instrument-corrected noise power spectra of pressure (P), vertical (Z) and horizontal (H⊥) motion. Units are Pa for $\dot{P}$ and μm for Z and H. (B) Coherency spectra, Z and P components, amplitude and phase of the data in A.; phase convention: P leads Z. (C) Same as 2B. but for Z and H⊥ components; +H⊥ is azimuth 246°; phase convention: H⊥ leads Z.

system required for installation in deep water. Corrected pressure spectra from the LP and SP (with the 3 Hz corner shifted to 0.3 Hz) hydrophones agree for phase and shape of amplitude between about 0.1 and 0.5 Hz (the overlapping frequency band), but the SP hydrophone data is about 6 dB higher than the LP hydrophone data; thus, the LP pressure power spectra presented in this paper may be up to 6 dB too low.

A final comment about the data: though one channel on both the LP and SP FM tapes measured compensation for wow and flutter during initial recording, we did not have the equipment to electronically compensate during playback. Instead, we subtracted the digitized compensation channel from each of the data channels and thereby improved data quality. Overall system noise limits background data above about 5 Hz and below about 0.003 Hz. (Except that the long-period horizontals record tilts down to at least 0.001 Hz.)

Results

Pressure and vertical velocity spectra, corrected for instrument response, are shown in Figure 1A. These spectra are calculated for a one hour period during which the bottom current velocity did not exceed 2 cm/sec. The pressure spectra agree with those obtained by Cox et al. [1984] and Webb and Cox [1986], showing a rapid decrease for frequencies below the "double frequency" microseism peak near .14 Hz to a strong minimum between about 0.03 and 0.1 Hz. At times, the "single frequency" microseismic noise, at about .06 Hz in this sample, is nearly absent, giving a deeper minimum. The pressure and vertical velocity spectra are generally similar except that the $P/\dot{Z}$ ratio increases significantly below about .02 Hz. The $P/\dot{Z}$ ratio for seismic waves is expected to decrease with decreasing frequency below about .07 Hz [Bradner, 1963] and appears to be correct for the .06 Hz peak. Below about .04 Hz $P/\dot{Z}$ is not consistent with predictions for seismic waves. H. Bradner and M. Reichle (personal communication) have obtained comparable results for the P and Z components of the OBSS between about 0.05 and 0.2 Hz for a different time period.

In Figure 1B the power spectrum from Figure 1A with SP vertical data added is compared with seismic noise on continents. Curves for continents represent noisy and quiet conditions on hard rock. [Similar curves for continents and islands are found in Murphy and Savino, 1975.] Between .06 and 5 Hz, the ocean bottom noise level pictured here is generally less than, but close to, the level of noisy continental data; below .04 Hz it is well above continental noise. The greatest

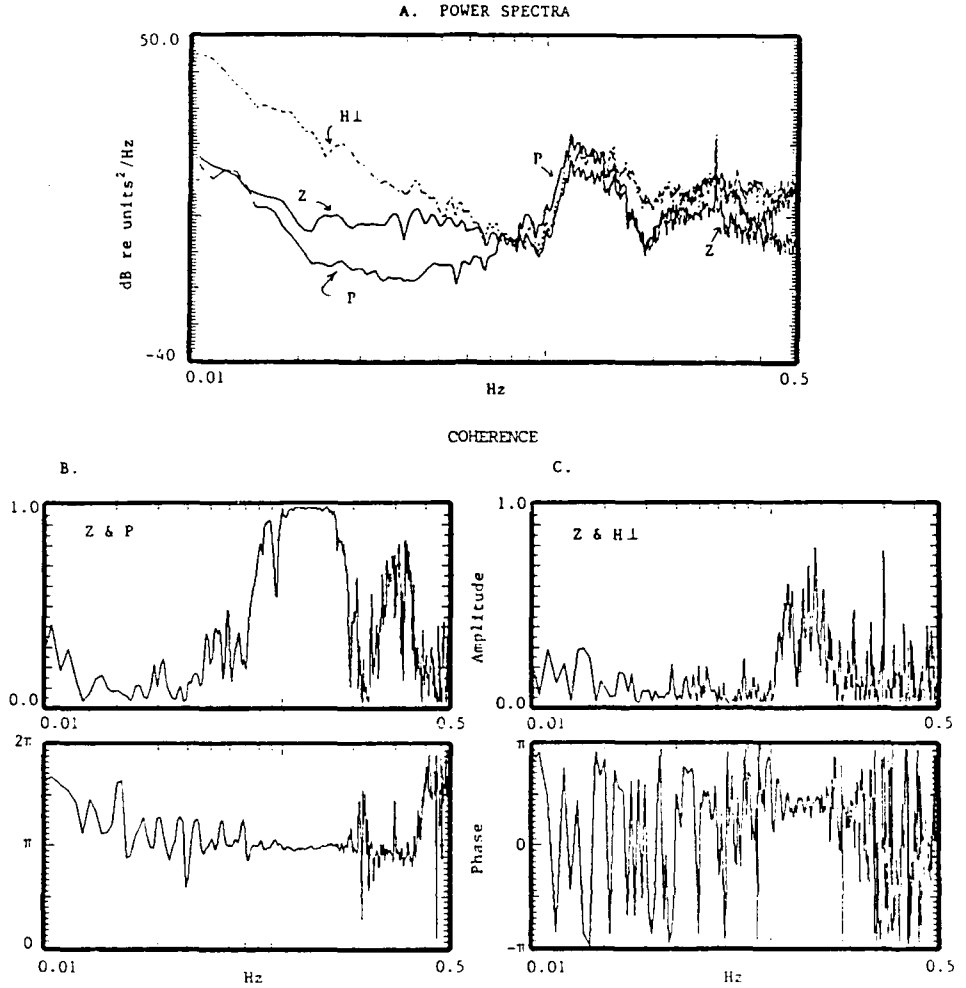

Fig. 3. (A) Instrument-corrected noise power spectra of pressure (P), vertical (Z) and horizontal (H⊥) motion. Units are Pa for P and μm for Z and H. (B) Coherency spectra, Z and P components, amplitude and phase of data in A. (C) Same as B. but for Z and H⊥ components. Phase conventions same as Figure 2.

"real" difference occurs near .01 Hz where the OBSS noise is over 32 dB above the "noisy" continental curve and it is possible that the "real" difference continues to decrease below .004 Hz. How much improvement would be obtained by better bottom-package design; shallow or deep burial within the bottom-sediment; or rigid coupling within the basalt of layer two are important questions to consider for the design of future OBS systems [e.g., Sutton and Duennebier, 1987]. The rise in spectral level at frequencies lower than the minimum is believed to be caused by ultra-long ocean waves and by meterological pressure disturbances on ocean-bottom and land stations, respectively [Webb and Cox, 1986; Murphy and Savino, 1975].

Power spectra and coherency among three components - pressure (P), vertical (Z), and horizontal motion perpendicular to shore (H⊥)- are calculated for two noise samples, 21 June and 4 July 1966 (Figures 2 and 3). The two samples illustrate time-variable features of microseismic noise. Strong coherency in Figure 2 near .06 Hz ("single frequency" microseisms) coincides with a peak in the power spectra of all three components. Between vertical displacement and pressure, coherency is strong from about .06 to .14 Hz and also at .30 Hz. Corrected phase relations and amplitude ratios for the spectral and coherency peaks near .06, .14, and .30 Hz are appropriate for fundamental mode Rayleigh waves. Theoretical results for appropriate velocity structures [Latham and Nowroozi, 1968] indicate that at .14 Hz fundamental mode Rayleigh waves are near the cross-over from retrograde (at the longer periods) to prograde particle motion. Thus, the observed phase relationship between Z and H⊥ indicates propagation toward shore at the OBSS location (about 160 km offshore) for the "single frequency" microseisms. Although Z - H⊥ amplitude coherency is not strong for the .14 and .30 Hz peaks, a stable phase coherency at .14 Hz indicates predominant $\pi/2$ phase difference, opposite the sign of the .06 peak. If the .14 Hz microseisms are prograde, their propagation is shoreward. The phase difference between Z and H⊥ around .30 Hz, though messy, looks more like $\pi/2$ than $-\pi/2$, again suggesting shoreward propagation of prograde fundamental Rayleigh waves. In contrast, the phase difference between Z and H⊥ in Figure 3 appears to be $-\pi/2$ which would indicate seaward propagation. The relatively poor coherency between Z and H⊥ for both the .14 and .30 Hz microseisms suggests variable propagation directions. Note also in Figure 3 that the "single frequency" microseism is not well developed.

In Figure 4 a P-Z coherency maximum near .01 Hz coincides with a spectral maximum most clearly observed from the hydrophone. The ratio of pressure to vertical velocity is much too high for fundamental mode Rayleigh waves. The amplitudes of these disturbances do not correlate in time with tidal currents but do correlate with ocean wave heights

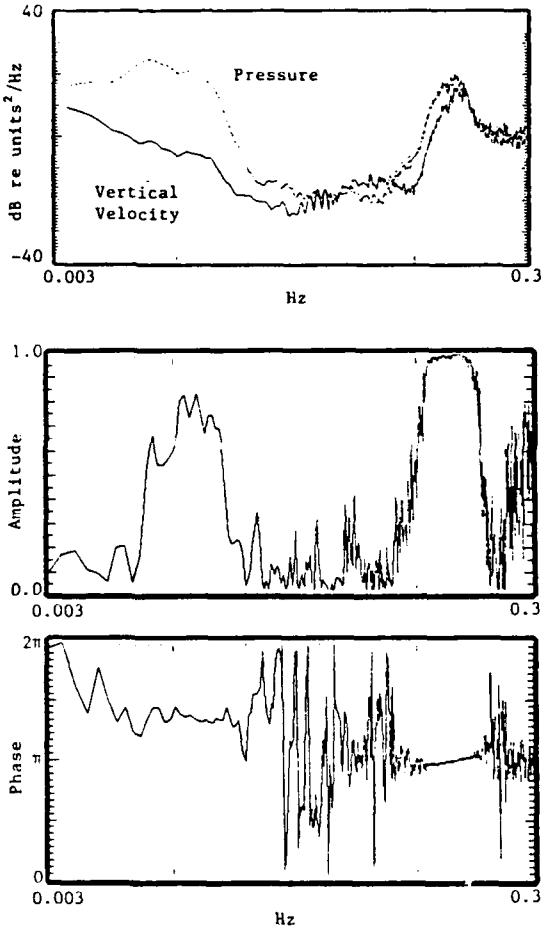

Fig. 4. Instrument-corrected noise power spectra and coherency spectra for Z and P components. Units are Pa for P and μm/sec for Z. Coherency spectra of the same data are calculated using vertical displacement; phase convention: P leads Z.

observed along the nearby California coast [Sutton et al., 1965]. The pressure signal is produced either by long (shallow water) waves non-linearly generated near shore from the ocean swell, or by differences in pressure beneath the high-amplitude vs. low-amplitude swell as varying amplitude wave-sets pass over OBSS, or a combination of the two. In the former case shoaling water is required, whereas in the latter case the disturbance would be observed wherever water depth is not large compared to the "wavelength" of the wave sets. In either case the velocities and wave lengths involved are much smaller than for seismic signals of the same period and the bottom moves as a forced deformation.

Summary

Results discussed is this paper are: 1) coherent spectral peaks are observed on vertical seismometers and hydrophones near .01, .06, .14, and .3 Hz; 2) the peak at .06 Hz also shows strong coherency with horizontal motion perpendicular to the coast; 3) peaks at .06, .14, and .30 Hz have comparable pressure-vertical velocity ratios and $\pi/2$ phase difference appropriate for free-running boundary waves; amplitude and phase relations, including horizontal components, suggest the .06 and .14 Hz peaks are predominantly fundamental mode Rayleigh waves propagating toward shore, but the .30 Hz peak is not as clear; 4) a peak at .01 Hz has 5-10 times greater pressure-vertical velocity ratio than shorter period peaks; the amplitude of the .01 Hz pressure peak correlates with ocean wave heights observed at nearby coastal stations; and 5) the noise spectra observed from the OBSS seismographs, including the deep (variable) minimum between about .03 and .1 Hz, are generally similar to published pressure spectra [e.g., Webb and Cox, 1986].

Acknowledgement. We thank Bob Bookbinder, Dave Lentricia, and Ellie Wellman at Lamont-Doherty Geology Observatory for helping make this research possible. This research was supported by the Office of Naval Research under contract # *N00014-86-C-0570*.

References

Auld, B., G. Latham, A. A. Nowroozi, and L. Seeber, Seismicity off the coast of northern California determined from ocean bottom seismic measurements, Bull. Seism. Soc. Am., 59, pp. 2001-2015, 1969.

Bradner, H., Probing sea-bottom sediments with microseismic noise, J. Geophys. Res., 68, pp. 1788-1791, 1963.

Cox, C., T. Deaton, and S. Webb, A deep-sea differential pressure gauge, Atmospheric and Ocean Technology, 1, pp. 237-246, 1984.

Latham, G. V. and A. A. Nowroozi, Waves, weather, and ocean bottom microseisms, J. Geophys. Res., 73, pp. 3945-3956, 1968.

Murphy, A. J. and J. M. Savino, A comprehensive study of long-period (20-200 sec) earth noise at the high-gain worldwide seismograph stations, Bull. Seis. Soc. Am., 65, pp. 1827-1862, 1975.

Nowroozi, A. A., M. Ewing, J. Nafe, and M. Fliegel, Deep ocean current and its correlation with the ocean tide off the coast of northern California, J. Geophys. Res., 73, pp. 1921-1932, 1968.

Nowroozi, A. A., J. Kuo, and M. Ewing, Solid earth and oceanic tides recorded on the ocean floor off the coast of northern California, J. Geophys. Res., 74, pp. 605-614, 1969.

Piermattei, R. and A. A. Nowroozi, Dispersion of Rayleigh waves for purely oceanic paths in the Pacific, Bull. Seism. Soc. Am., 59, pp. 1905-1925, 1969.

Sutton, G. H., W. G. McDonald, D. D. Prentiss, and S. N. Thanos, Ocean-bottom seismic observatories, Proceedings of the IEEE 53, pp. 1909-1921, 1965.

Sutton, G. H. and F. K. Duennebier, Optimum design of ocean bottom seismometers, Marine Geophys. Res., 9, pp. 47-65, 1987.

Webb, S. C. and C. S. Cox, Observations and modeling of seafloor microseisms, J. Geophys. Res., 91, pp. 7343-7358, 1986.

N. Barstow, J. A. Carter, and G. H. Sutton, Rondout Associates, Incorporated, P.O. Box 224 Stone Ridge, NY 12484.

(Received: April 10, 1989;
Accepted: July 25, 1989.)

APPENDIX B

OCEAN-BOTTOM ULF SEISMO-ACOUSTIC AMBIENT NOISE: .002 to .4 Hz

George H. Sutton and Noël Barstow
Rondout Associates, Incorporated
P.O. Box 224
Stone Ridge, NY 12484

To be published in the
April, 1990 Number of the Journal of the Acoustical Society of America

Abstract

Observed spatial and temporal characteristics of ULF ocean-bottom seismo-acoustic ambient noise are required in order to construct realistic quantitative predictive models of the phenomena involved. Few such data exist or have been studied, especially for frequencies below about 0.1 Hz. We present analysis of noise data in the band .002 to .4 Hz from a two-week period, 11/28 to 12/12/67, recorded from long-period, 3-component seismometers and a hydrophone of the Columbia-Point Arena ocean-bottom seismic station (OBSS, 38° 09.2'N - 124° 54.4'W, 3903 m depth). Two intense NE Pacific storms with hurricane force winds occurred during the emphasized time period. Time variations of spectra and of amplitude and phase coherencies of the 4-component OBSS data are related to the storm histories and to local weather/wave conditions and are used to identify motion (seismic wave) types and directions of propagation.

Introduction

The general objective of this research is to improve our quantitative understanding of the ambient acoustic/seismic noise field in the ocean as a function of location and time in the ULF (0.001 to 1 Hz)/VLF (1 to 50 Hz) frequency band by identifying and characterizing the noise sources and determining the propagation characteristics of the ambient noise field as functions of the ocean and sub-bottom environmental parameters. The specific research reported here characterizes ULF ocean bottom noise during two northeast Pacific storms, measured at a single multi-sensor station.

The most extensive set of ocean bottom data on long period seismic background noise and signals was obtained from the Columbia-Point Arena Ocean Bottom Seismic Station (OBSS, Sutton *et al.*, 1965). OBSS was installed on 18 May, 1966 at 38° 09.2'N, 124° 54.4'W about 200 km west of San Francisco at a depth of 3903 meters and it was in continuous operation for more than six years, until 11 September 1972. Though a number of papers

(e.g. Auld *et al.*, 1969; Latham and Nowroozi, 1968; Piermattei and Nowroozi, 1969; Sutton *et al.*, 1965; Nowroozi *et al.*, 1968 and 1969) have been published using OBSS data, little had been published on the background noise, especially outside the principal microseism band, .1 to .2 Hz, until recent interest in ULF/VLF noise led us to examine OBSS data specifically for this information. OBSS instruments primarily used for this study are the Lamont long-period (LP) triaxial seismometer (15 sec natural period, originally developed for lunar use) and the long-period (crystal) hydrophone. Records from the three-component short-period (SP) system (1 sec natural period) and short-period (coil-magnet) hydrophone also were consulted. We digitized FM tapes of the long-period data at 8 sps.

We present analyses of OBSS seismo-acoustic ULF data for a two week period, 11/28 to 12/11/67, during which two NE Pacific storms with hurricane force winds occurred. Samples of ocean bottom noise in the frequency band 0.002 to 0.4 Hz are analyzed for coherency and amplitude and phase relationships among the three components of particle motion and pressure.

Results

Figure 1 shows the location and the orientation of the horizontal components of OBSS and the tracks of the two storms studied. Maximum intensities of storm activity occurred between about 1200 UT 12/1 and 1800 UT 12/2 for the earlier storm and between about 1200 UT 12/5 and 0000 UT 12/6 for the later storm (Mariners' Weather Log, 1968). From 11/30 through 12/8 (except 12/2) swell height near OBSS was greater than 15 feet and on 11/30 and 12/3-12/5 combined sea and swell was greater than 20 feet (historical conditions obtained from Pacific Weather Analysis). For the period 11/28 to 12/11/67 we digitized, somewhat arbitrarily, 6-, 12-, or 4-hour samples of noise (Figure 2). These samples of ocean bottom noise are used to determine spectra, coherency, and amplitude and phase relationships among the three components of particle motion and pressure in the frequency band .002 to 0.4 Hz.

Below about .003 Hz some low amplitude samples may be affected by system noise.

The pressure spectra generally agree with those obtained by Cox *et al.* (1984) and Webb and Cox (1986) showing a strong minimum between about 0.03 and 0.1 Hz referred to as the "noise notch"; motion spectra from the OBSS seismometers, especially the vertical sensor, are qualitatively similar to the pressure spectra (Figure 3). Figure 3 shows velocity and pressure spectra from three different times: time 1 (0200 UT 11/28) is before the storms; time 2 (1200 UT 12/4) occurs after the peak in double-frequency (twice ocean swell frequency) microseisms associated with storm 1; and time 3 (0200 UT 12/8) is near the peak double-frequency microseisms associated with storm 2. It can be seen that the whole spectral level between .003 and .4 Hz is raised for both vertical velocity, $\dot{Z}$, and pressure, P. For frequencies below about .08 Hz the horizontal components are affected more by local tidal currents (most likely from direct turbulent pressure on the OBSS package, Sutton, 1986; Sutton and Duennebier, 1987 and 1989) than by the storm activity.

The data divide naturally into five frequency bands (.004-.02 Hz, .02-.04 Hz, .04-.08 Hz, .08-.2 Hz, and .2-.4 Hz) based upon observed characteristics and upon assumed mode of origin and/or propagation. The band divisions are labeled in Figure 4, where amplitude and phase coherency between pressure and vertical motion are shown. Below we discuss each band separately.

1. Band .004-.02 Hz: In this band it is believed that the pressure variations result from long gravity water waves having wavelengths greater than water depth but much less than seismic waves of the same frequency (Webb and Cox, 1986; Webb, 1988; Barstow *et al.*, 1989). Webb and Cox (1986) predict that this band should be fairly constant with time; however, we observe an increase in P and Z near .01 Hz of about 20 dB during the storms (Figure 3). Sutton *et al.* (1965) also found a temporal correlation with ocean wave heights along the nearby (to OBSS) California coast. The pressure disturbance should produce a forced deformation of the bottom and near .01 Hz we observe a strong correlation between P and Z in

Figures 4 and 5. Yamamoto and Torii (1986) use such correlated pressure and motion in shallow water to estimate rigidity vs. depth in the sub-bottom as a function of gravity wavelength (period). This theory assumes that variations are slow enough that static loading theory is adequate. The approximately $3\pi/2$ phase between vertical displacement and pressure (maximum pressure in phase with maximum downward velocity) observed in Figure 4 indicates that dissipation (radiation) is involved and that the static theory is not adequate. Static theory would predict π phase (maximum pressure in phase with maximum downward displacement) as is also the case for Rayleigh waves. The pressure-vertical velocity ratio ($P/\dot{Z}$) near .01 Hz is 24 dB ± 2.7 S.D. for 21 samples, much too large for fundamental mode Rayleigh waves. All $P/\dot{Z}$ ratios were obtained by graphical measurement of individual power spectra calculated from one-hour samples divided into 8 Hanning windows with 62.5 % overlap.

2. Band .02-.04 Hz: In this band we observe poor P-Z coherence (Figures 4 and 5). The $P/\dot{Z}$ ratio near .02 Hz is 13.2 dB ± 6.2 S.D. for 21 samples. This average is well above that expected for seismic waves. Near .04 Hz, however, some samples have ratios appropriate for fundamental mode Rayleigh waves (LR). During the storm, amplitudes near .04 Hz increased 10-20 dB (Figure 3). In this band, which is partially within the .03-.1 Hz "noise notch", some low amplitude samples may be system noise limited.

3. Band .04-.08 Hz: P-Z coherence is variable in this band, which is also within the .03 -.1 Hz "noise notch" (Figures 4 and 5). During the storm, amplitudes near .06 Hz increased 10-15 dB. The $P/\dot{Z}$ ratio near .06 Hz for 21 samples is 6.8 dB ± 3.1 S.D.; again, some low-amplitude samples may be system noise limited. The highest amplitude samples (Figure 7) have amplitude and phase relationships consistent with fundamental mode Rayleigh waves.

This is the frequency band of single-frequency microseisms and of prominent oceanic Rayleigh waves from earthquakes. The single- frequency microseisms are generally believed to be produced from direct pressure of shoaling swell in coastal areas and have been observed mostly on land instruments (Oliver, 1962; Oliver and Page, 1963; Haubrich and McCamy,

1963; Cessaro and Chan, 1989). Consistent with this are Webb and Constable's (1986) interpretation of ambiguous results from a two element ocean-bottom array as indicating Rayleigh propagation from near shore. Spectra (peaking near .06 Hz) and coherencies observed from June 1966 OBSS data by Barstow *et al.* (1989), however, clearly indicate fundamental mode Rayleigh waves propagating shoreward rather than seaward as would be expected from generation near the California coast.

Webb and Cox (1986) noted the transient nature of spectral peaks for ocean-bottom single-frequency microseisms compared to more stable double-frequency microseisms. We observe generally strong but variable P-Z coherency during the 11/28 - 12/11/67 time period, but there are few clear spectral peaks in this bandwidth. However, within the three-hour period of high P-Z coherency near .06 Hz (0200-0500 UT 12/8, Figure 5), we are able to observe single-frequency microseisms by narrow band-pass filtering the seismograms (Figure 6). These microseisms, peaked at .05-.06 Hz, have proper amplitude and phase relationships for LR and indicate shoreward (from 260°) propagation, as did our earlier results (Barstow *et al.*, 1989). Also, we do not observe a precise 2 to 1 frequency relationship with the observed double-frequency microseisms as would be expected if the same swell produced both types. Oliver and Page (1963) and Haubrich and McCamy (1963), for example, at land stations observed a quite accurate 2 to 1 relationship.

4. Band .08-.2 Hz: This is the band of the prominent double-frequency microseisms. We observe high P-Z coherency and a large increase in amplitude (30-40 dB) and an increase in period during the storms (Figures 2 and 3). The $P/\dot{Z}$ ratio near .1 Hz is 15.2 dB ± .8 S.D. for 21 samples. The amplitude and phase relationships in this band indicate fundamental mode Rayleigh waves propagating shoreward assuming prograde motion based on an appropriate velocity structure (Latham and Nowroozi, 1968; Bradner and Latham, 1972). The evidence, least ambiguous for double-frequency microseisms, is as follows. (The same kinds of data and reasoning were used to characterize single-frequency microseisms and will be

discussed for wind-wave microseisms.) The π phase difference between pressure and vertical displacement is correct for Rayleigh wave motion and, though shown only in Figure 4, we have observed it in all the coherence spectra between roughly .04 and .4 Hz (except at .08 and .2 Hz). The $P/\dot{Z}$ amplitude ratios from .04-.15 Hz are consistent with fundamental mode Rayleigh waves for several reasonable velocity models (Figure 7). The theoretical points on the $P/\dot{Z}$ ratio plots in Figure 7 are from models 5 and 8 of Bradner, 1963. These models are probably the closest of those shown in Figure 7 to the structure at OBSS (e.g. Sutton *et al.*, 1971); model values are given in the table below.

Bradner (1963) Models 5 and 8

Model#	H,km	ρ,g/cm^3	V_s,km/sec	V_p,km/sec
5	6	1.03		1.52
	1	1.03	0.5	1.52
	6	2.75	3.98	6.9
	∞	3.09	4.68	8.1
8	6	1.03		1.52
	0.5	1.03	0.25	1.52
	1.5	2.54	2.77	4.8
	5	2.75	3.98	6.9
	∞	3.09	4.68	8.1

The H/Z amplitude ratios are also consistent with fundamental mode Rayleigh waves (Figure 8). Velocity models appropriate for the OBSS site indicate prograde particle motion for LR at frequencies higher than about .1 Hz. Assuming prograde motion, then, the double-frequency microseisms are propagating shoreward (Figure 9). In Figure 9 the vertical to horizontal coherencies and transfer functions are used to determine the propagation direction of Rayleigh waves. The phase coherencies determine the appropriate quadrant and the ratio of the transfer functions determines the angle relative from HII (Figure 1). Between .09 and .15 Hz (double frequency) propagation is from the west (275°). In the same manner, we determined a propagation direction of 260° for single-frequency microseisms near .06 Hz where fundamental mode LR is retrograde.

The relationship between the storms and the timing of changes in double-frequency microseisms is a clue to microseism origin. Using the distance to OBSS of the closest approach of hurricane force winds generated in storm 1 (Figure 1), the calculated arrival time for 17 sec water waves is 1200 UT on 12/3. Similarly for storm 2, the calculated arrival time is 2000 UT on 12/7. The earlier of two observed maxima for 8 1/2 sec microseisms occurs at about 1200 UT 12/3 (Figure 2) as predicted for generation near OBSS from interfering 17 sec swell of storm 1. The later-occurring maximum period and amplitude of double- frequency microseisms is observed early on 12/8, somewhat later than predicted for swell to reach OBSS from the distances of hurricane force winds associated with storm 2. It is important to our understanding of the generation of double-frequency microseisms that the observed high-amplitude, longest-period arrivals from both storms are later than expected for Rayleigh waves generated either near the storm center or at the coastal areas nearest the storm center. Thus the time delay relative to the storm activity suggests double-frequency microseism generation near OBSS. We do not have a simple explanation for the two-to-three-day cycle of double-frequency amplitude variations in Figure 2. From 11/30 to 12/8 the low-amplitude values steadily increase, and then on 12/10 drop back to pre-storm low levels. The pattern of high-amplitude values is puzzling, yet the two longest-period peaks in amplitude sensibly relate to the storm tracks.

There have been many investigations, mostly involving only land observations, of double-frequency microseisms. They are generally believed to be generated by non-linear wave-wave interaction either near a storm center or upon reflection from a coastline. Our ocean bottom data seem to require interaction offshore and away from the storm center. Perhaps the double-frequency microseisms from both storms are a result of interference between direct arriving storm swell and reflections off northern California and Oregon (Figure 1).

5. Band .2-.4 Hz: Figure 5 shows a stable P-Z coherency maximum near .3 Hz and a

minimum near .2 Hz separating it from the main double-frequency maximum. Amplitudes at .3 Hz varied up to 20 dB during the storms. Pressure and velocity amplitude fluctuations in this band correlate well with local wind and weather conditions; the generation of these microseisms is related to wind waves. On the original short-period photographic records, we observed two pronounced amplitude maxima, 12/3 and 12/7. These coincide with the two maxima in local winds identified by Pacific Weather Analysis for the two week period studied: 30 knots and above from the southeast and the northwest, respectively. The $P/\dot{Z}$ ratio near .3 Hz is 6.9 dB ± 1.0 S.D. for 16 samples. We note that observed $P/\dot{Z}$ ratios above about .15 Hz do not match fundamental mode theory well (Figure 7). Higher modes change amplitude ratio and particle motion over narrow bandwidths and are highly sensitive to velocity structure, making it difficult to assess their propagation direction. If particle motion is prograde, propagation is seaward, i.e. from Figure 9, near .33 Hz propagation is from the east (100°). Relatively poor coherency between vertical and horizontal ground motion, however, suggests variable propagation direction.

Summary

The pressure spectra are similar to those obtained by Cox *et al.* (1984) and Webb and Cox (1986) showing two maxima separated by a strong minimum between about 0.03 and 0.1 Hz; motion spectra from the OBSS seismometers, especially the vertical sensor, are similar to the pressure spectra. Coherent energy from 0.1-0.15 Hz and intermittently near 0.06 Hz indicate fundamental mode Rayleigh wave motion propagating shoreward. The timing of high amplitude, longer-period double-frequency microseisms is consistent with microseism generation near OBSS rather than closer to the storm center. Background noise levels around .06 Hz, are intermittently coherent between P and Z during the two week period of this study, but rarely do they produce spectral peaks. Coherent energy near .3 Hz is consistently high and the highest amplitudes correspond to the highest local winds for the period. The $P/\dot{Z}$ ratios show that these wind-wave microseisms are not fundamental mode Rayleigh waves.

Coherent energy near .01 Hz varies with time, but is well above random coherency (estimated from coherency between samples of P and Z taken at separate times). Another result from both our previous study of fairly quiet conditions (Barstow *et al.*, 1989) and the current study of severe storm conditions is a 90° phase shift near .01 Hz between pressure and vertical displacement, indicating dissipation or radiation, in the forced deformation of the bottom from long gravity water waves.

Acknowledgment

We gratefully acknowledge: Lamont-Doherty Geologic Observatory for providing the original data, and Hugh Bradner, Leroy Dorman, Paul Pomeroy, and Jerry Carter for their interest and useful comments regarding this research. The Office of Naval Research supported this research under Contract No. N00014-86-C-0570.

REFERENCES

Auld, B., G. Latham, A. A. Nowroozi, and L. Seeber, "Seismicity off the coast of northern California determined from ocean bottom seismic measurements," *Bull. Seism. Soc. Am.*, vol. 59, pp. 2001-2015, 1969.

Barstow, N., G. H. Sutton, and J. A. Carter, "Particle motion and pressure relationships of ocean bottom noise at 3900 m depth: 0.003 to 5 Hz," *Geophys. Res. Let.*, vol. 16, pp. 1185-1188, 1989.

Bradner, H., "Probing sea-bottom sediments with microseismic noise," *J. Geophys. Res.*, vol. 68, pp. 1788-1791, 1963.

Bradner, H. and G. V. Latham, "Prograde Rayleigh waves and microseism sources," *J. Geophys. Res.*, vol. 77, pp. 6422-6426, 1972.

Cessaro, R. and W. Chan, "Wide-angle triangulation array study of simultaneous low-frequency microseism sources," *J. Geophys. Res.*, 1989 (in press).

Cox, C., T. Deaton, and S. Webb, "A deep-sea differential pressure gauge," *Atmospheric and Oceanic Technology*, vol. 1, No. 3, pp. 237-246, 1984.

Haubrich, R. A. and R. L. McCamy, "Microseisms: coastal and pelagic sources," *Rev. Geophys.*, vol. 7, pp. 539-572, 1963.

Latham, G. V. and A. A. Nowroozi, "Waves, weather, and ocean bottom microseisms," *J. Geophys. Res.*,, vol. 73, pp. 3945-3956, 1968.

Mariners Weather Log, *U.S. Dept. of Commerce, NOAA, Environmental Data Source (U.S. Government Printing Office)*, Washington, D.C., 1968.

Nowroozi, A. A., M. Ewing, J. Nafe, and M. Fliegel, "Deep ocean current and its correlation with the ocean tide off the coast of northern California," *J. Geophys. Res.*, vol. 73, pp. 1921-1932, 1968.

Nowroozi, A. A., J. Kuo, and M. Ewing, "Solid earth and oceanic tides recorded on the ocean floor off the coast of northern California," *J. Geophys. Res.*, vol. 74, pp. 605-614, 1969.

Oliver, J., "A worldwide storm of microseisms with periods of about 27 seconds," *Bull Seism. Soc. Am.*, vol. 52, pp. 507-518, 1962.

Oliver, J. and R. Page, "Concurrent storms of long and ultralong period microseisms," *Bull. Seism. Soc. Am.*, vol. 53, pp. 15-26, 1963.

Piermattei, R. and A. A. Nowroozi, "Dispersion of Rayleigh waves for purely oceanic paths in the Pacific," *Bull . Seism. Soc. Am.*, vol. 59, pp. 1905-1925, 1969.

Sutton, G. H., W. G. McDonald, D. D. Prentiss, and S. N. Thanos, "Ocean-bottom seismic observatories," *Proceedings of the IEEE*, vol. 53, No. 12, pp. 1909-1921, 1965.

Sutton, G. H., G. L. Maynard, and D. M. Hussong, "Widespread occurrence of a high-velocity basal layer in the Pacific crust found with repetitive sources and sonobouys," *The Structure and Physical Properties of the Earth's Crust*, pp. 193-209, John G. Heacock, ed., 1971.

Sutton, G. H., "Ocean bottom seismology: history and current status," *Ocean Seismo-acoustics*, pp. 821-840, T. Akal and J. M. Berkson, ed., Plenum, 1986.

Sutton, G. H. and F. K. Duennebier, "Optimum design of ocean bottom seismometers," *Marine Geophys. Res.*, vol. 9, pp. 47-65, 1987.

Sutton, G. H. and F. K. Duennebier, "Avoiding signal distortion and excess noise in OBS," *Proceedings of Workshop on Exploration of Deep Continental Margin Crust with Closely Spaced Shots and Receivers*, pp. A21-A22 (with 4 pp. of figures), M. Talwani, P. L. Stoffa and W. D. Mooney, ed., 1989.

Webb, S. C. and S. C. Constable, "Microseism propagation between two sites on the deep seafloor," *Bull. Seism. Soc. Am.*, vol. 76, pp. 1433-1446, 1986.

Webb, S. C. and C. S. Cox, "Observations and modeling of seafloor microseisms," *J. Geophys. Res.*, vol. 91, pp. 7343-7358, 1986.

Webb, S. C., "Long-period acoustic and seismic measurements and ocean floor currents," *J. Ocean. Eng. (I.E.E.E.)*, vol. 13, pp. 263-270, 1988.

Yamamoto, T. and T. Torii, "Seabed shear modulus profile inversion using surfacing gravity (water) wave-induced bottom motion," *Geophys. J. Roy. Astr. Soc.*, vol. 85, pp. 413-431, 1986.

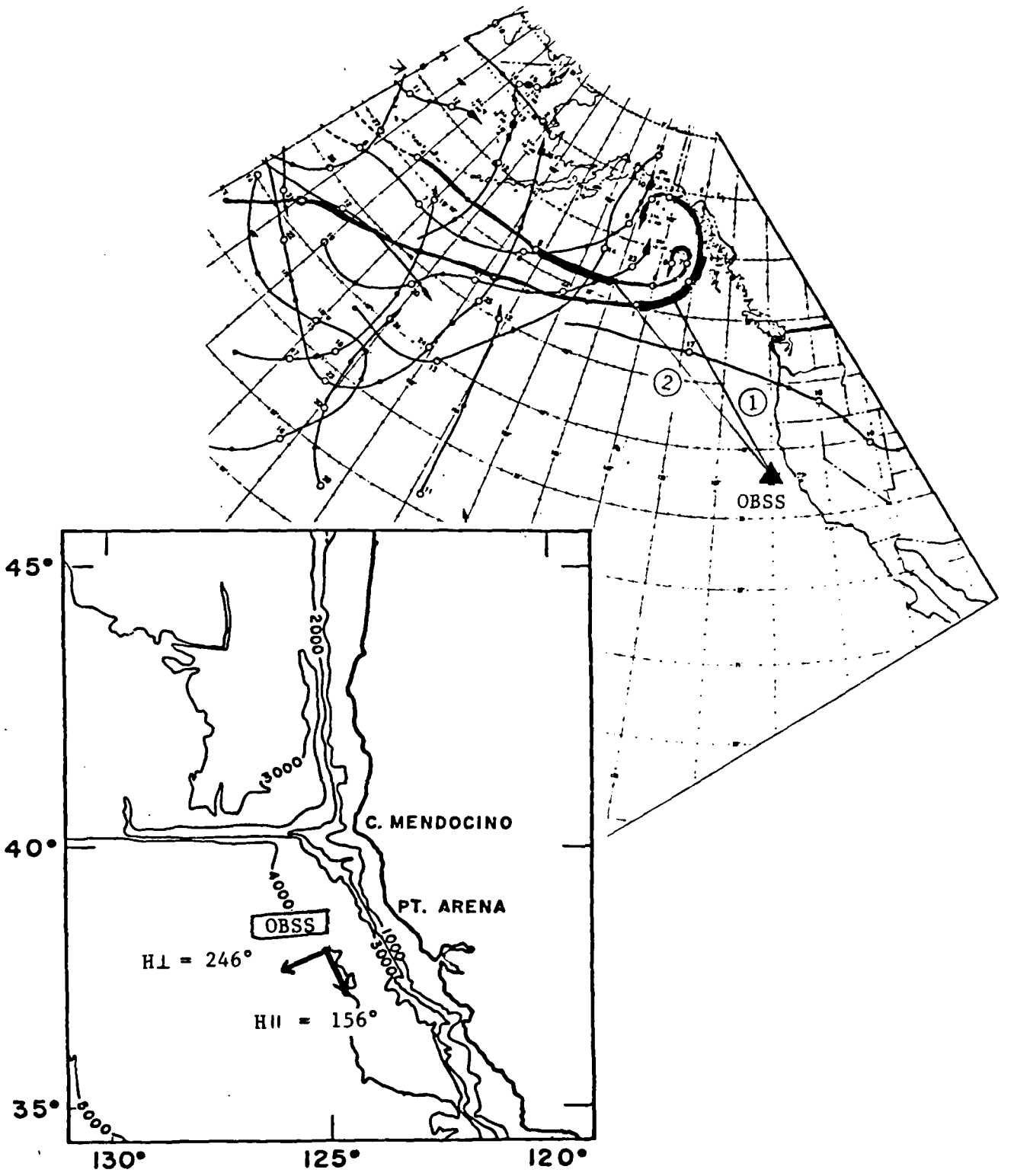

Figure 1. Location and orientation of OBSS and tracks of two 1967 hurricanes. Thickened lines show duration and location along the storm tracks of hurricane force winds. Storm 1 (11/29-12/5); closest approach of center of hurricane winds, Δ=15.7°. Storm 2 (12/3-12/8); closest approach of hurricane winds, Δ=19.3°.

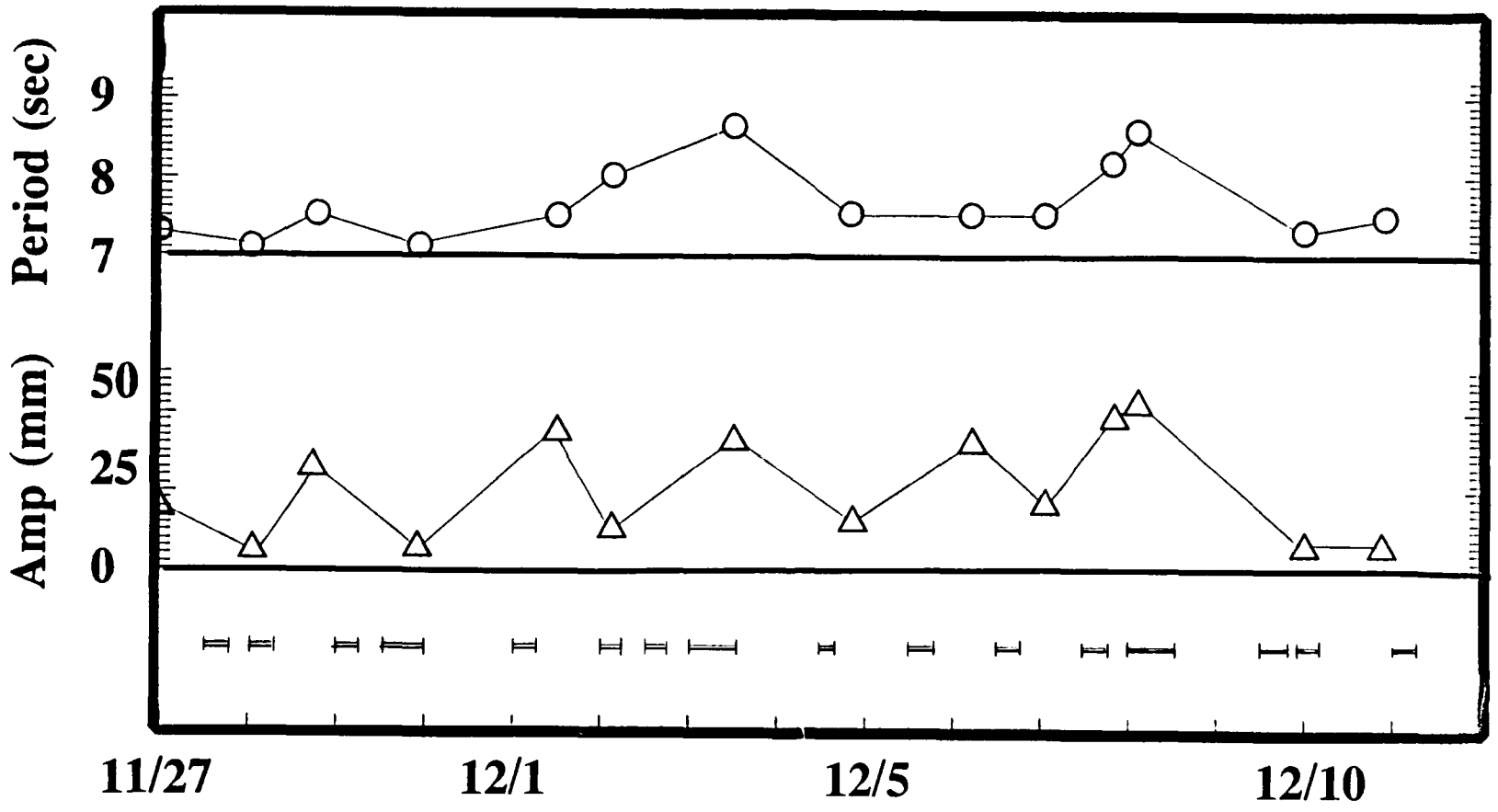

Figure 2. Measured from the original long-period photographic, continuous analog records are predominant period (circles) and average peak-peak trace amplitude (triangles) for vertical component microseismic background noise during times of amplitude maxima and minima (usually lasting several hrs). Horizontal bars represent time samples of background noise digitized from original FM tapes.

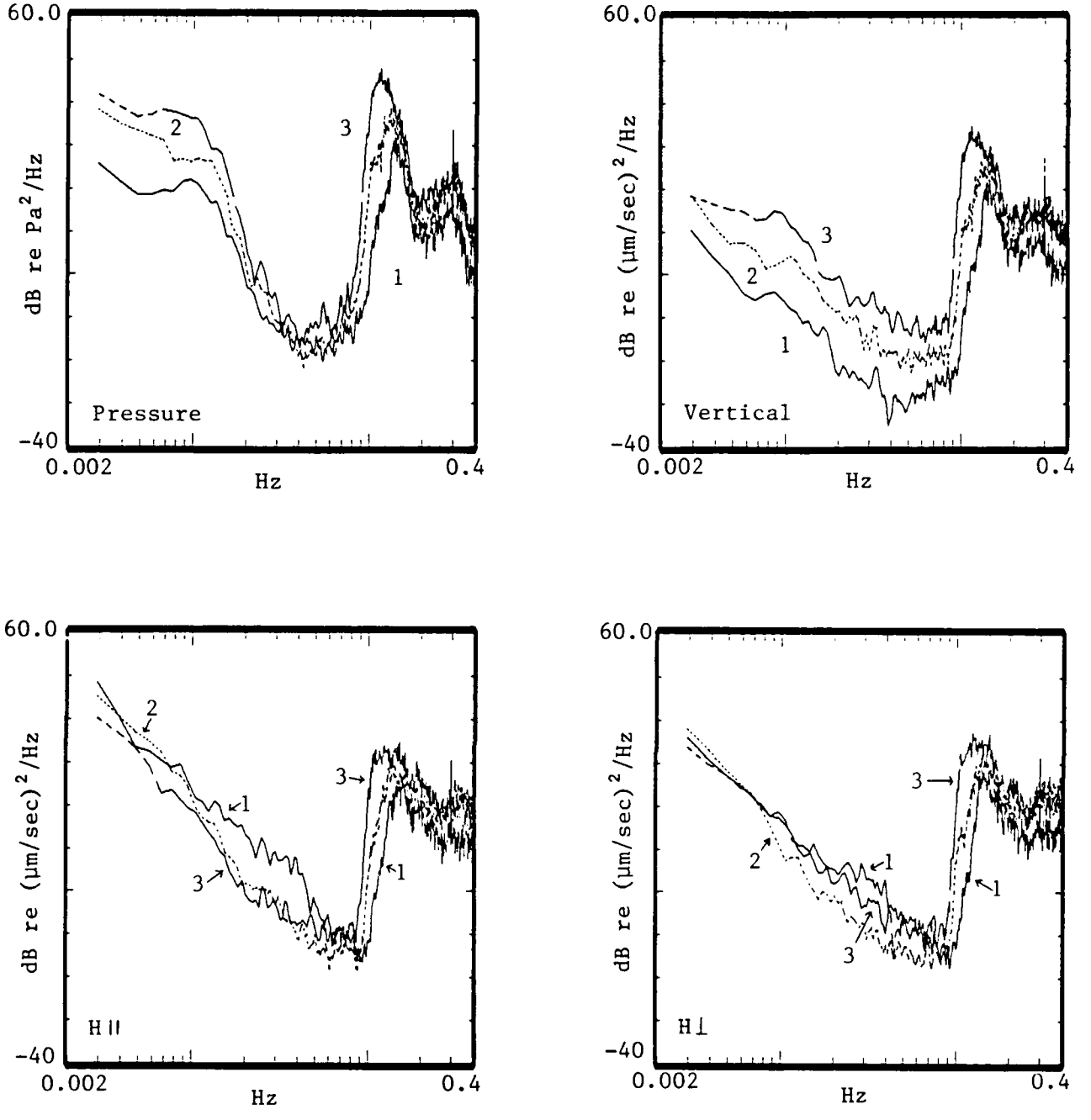

Figure 3. Pressure and three-component velocity power spectra from three time periods: 1 before (11/28), 2 during (12/4), and 3 near a peak (12/8) in microseism storm activity associated with two NE Pacific hurricanes in December 1967. Note that the whole spectrum is raised for pressure and vertical motion and only that above .08 Hz for horizontal motion. Spectra were calculated from one-hour samples divided into 8 Hanning windows with 62.5% overlap.

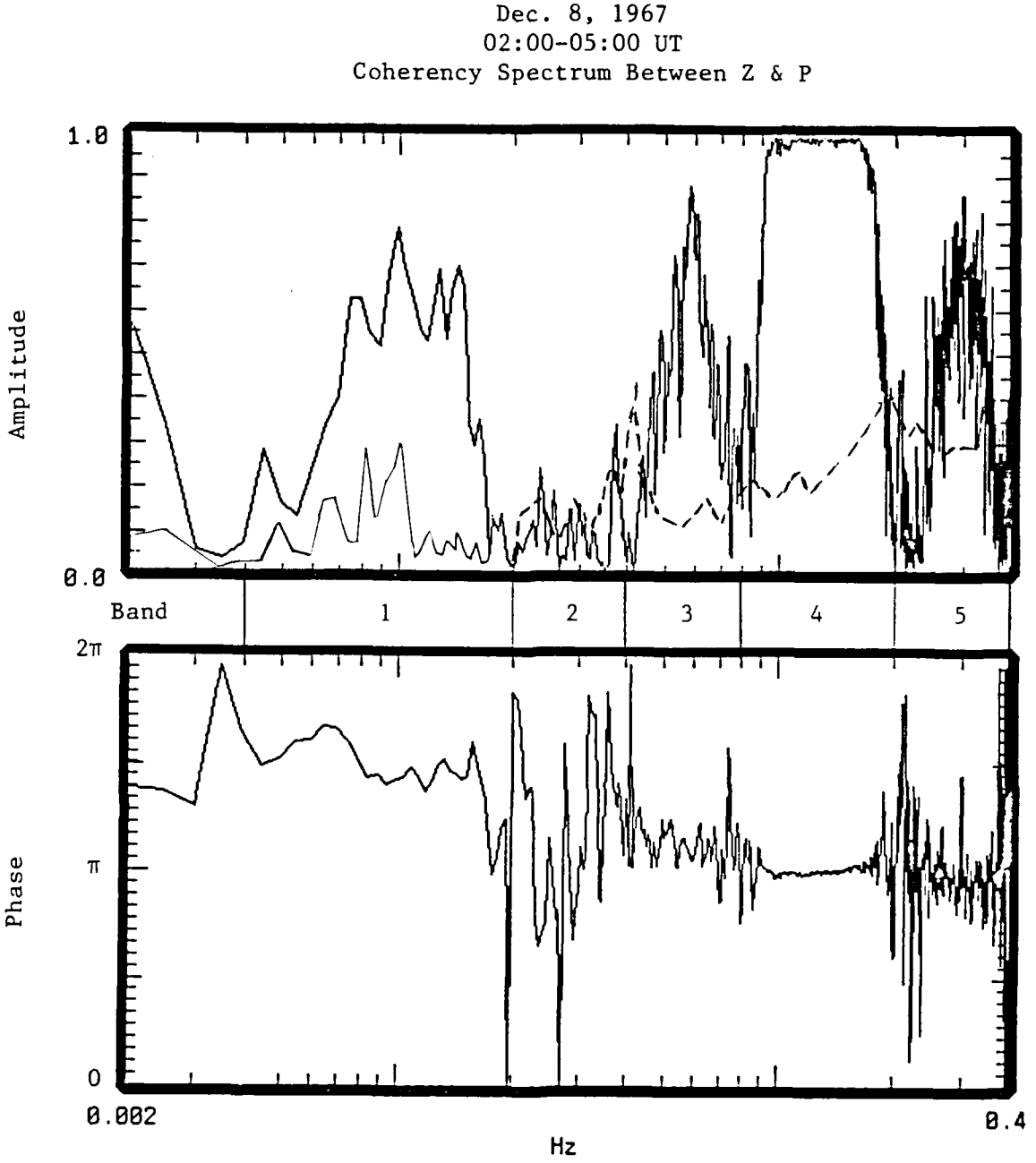

Figure 4. Amplitude and phase coherency between vertical displacement and pressure during peak of microseism storm. An estimate of random amplitude coherency is given by the generally, lower-amplitude spectrum obtained between samples of P and Z taken at separate times; above .02 Hz the dashed line connects the largest maxima in the spectrum. π phase (maximum pressure in phase with maximum down displacement) is correct for Rayleigh wave motion. $3\pi/2$ phase near .01 Hz (maximum pressure in phase with maximum down velocity) is not consistent with simple static loading from long gravity water-waves. Numbered frequency bands correspond to text. This and succeeding coherency spectra were calculated from 3 Hr. samples divided into 16 Hanning windows with 62.5% overlap.

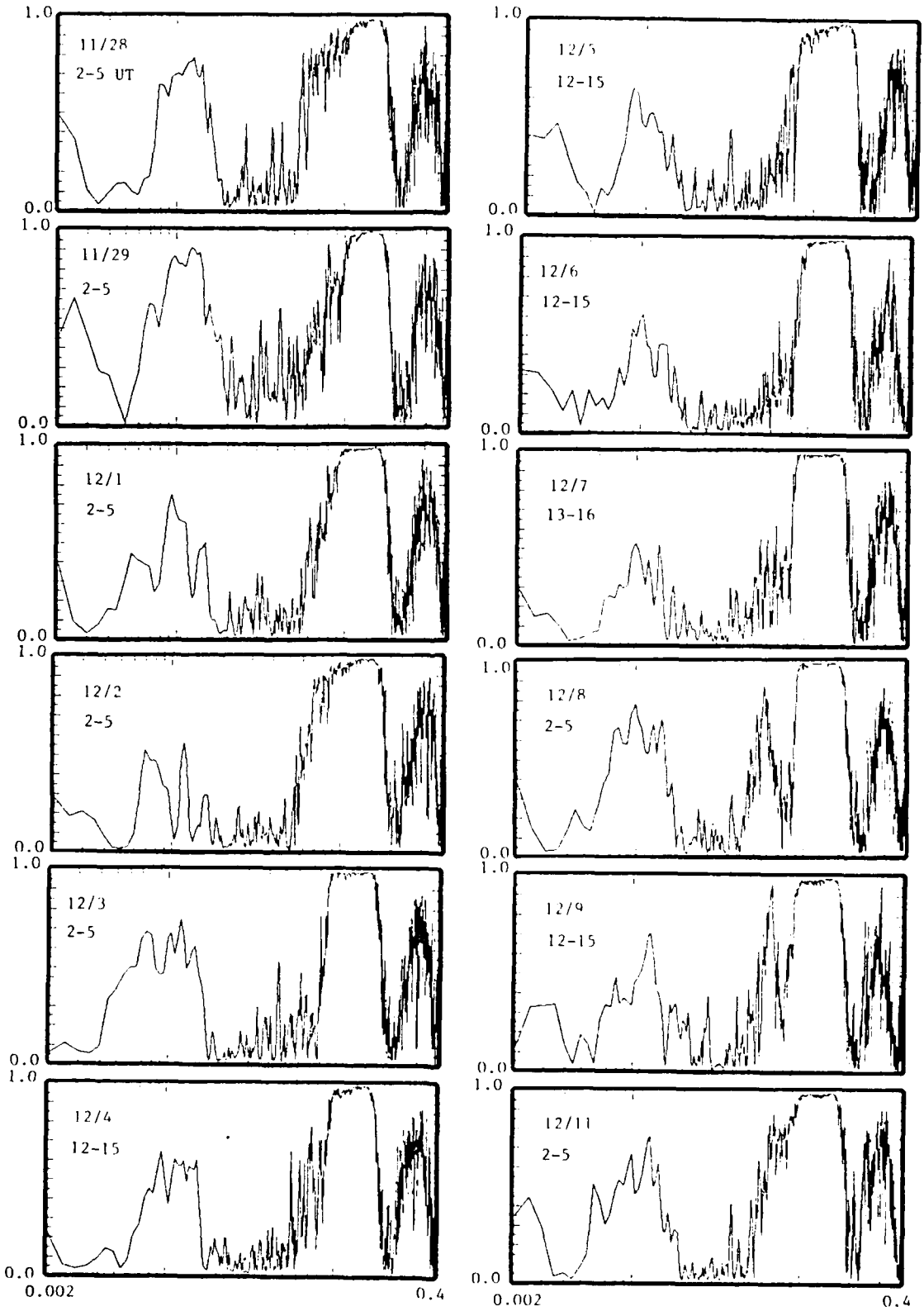

Figure 5. Amplitude coherency between pressure and vertical motion (.002 to .4 Hz) during two week period including two hurricanes. Note the variable coherency in the 'single frequency' microseism band between about .05 and .1 Hz and the consistently low coherency near 0.2 Hz and also from .02-.04 Hz.

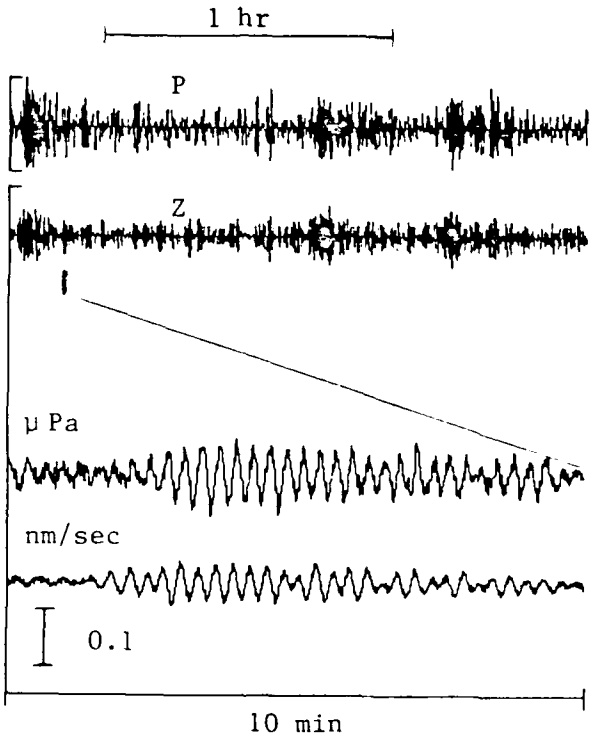

Figure 6. Pressure and vertical velocity band-pass filtered from .04-.06 Hz to enhance single-frequency microseisms; all traces start at 0300 UT on 12/8. Amplitude scale applies only to time-expanded traces, for which pressure is plotted positive downward.

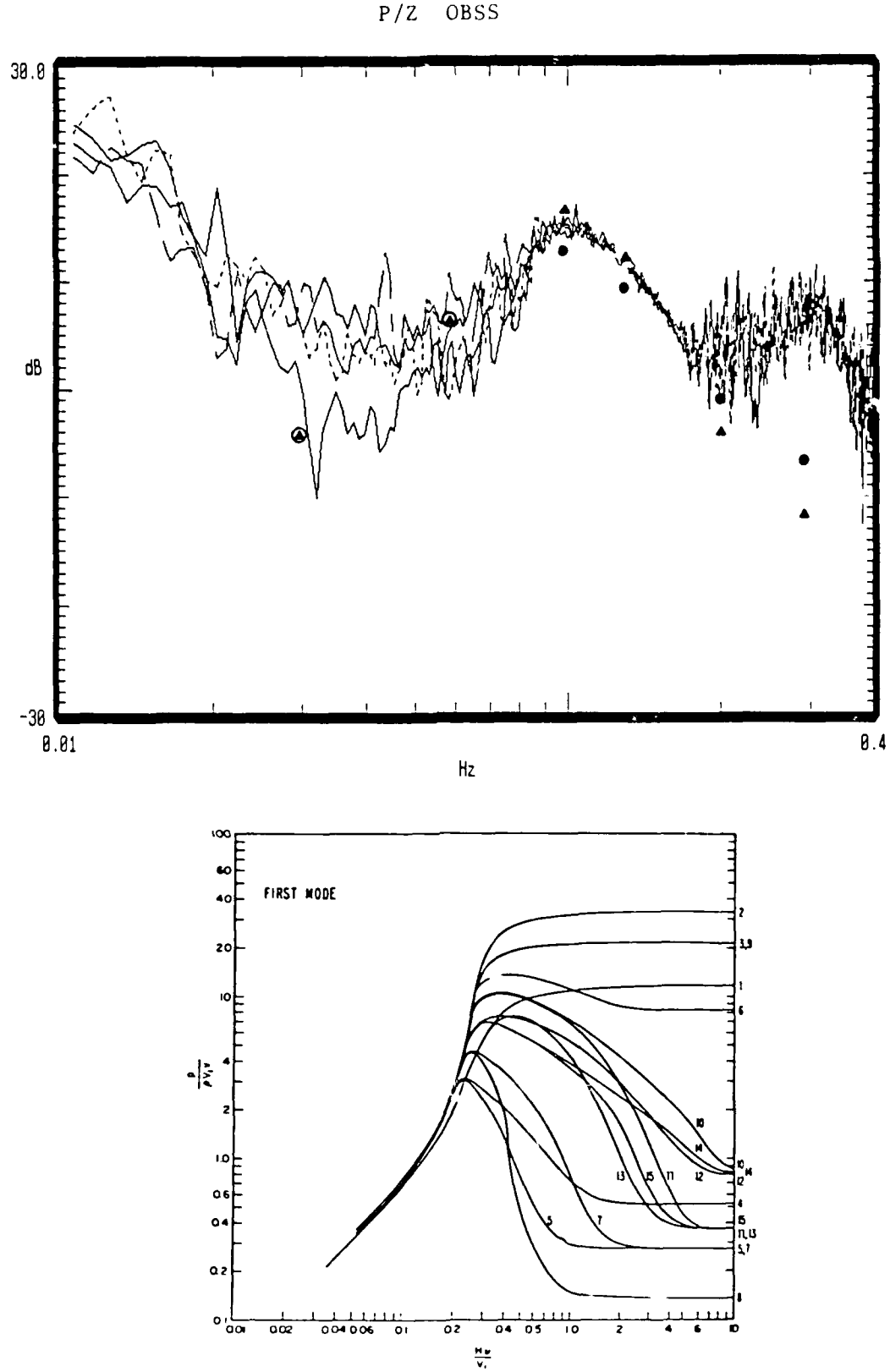

Figure 7. Pressure-vertical velocity ratio for four time periods (12/2,3,5,8) when both P and Z are at least 6dB above the lowest recorded levels (i.e., little or no system noise). Theoretical curves are fundamental Rayleigh for different velocity models (Bradner, 1963). Triangles and circles on data plot are for models 8 and 5, respectively (Table 1).

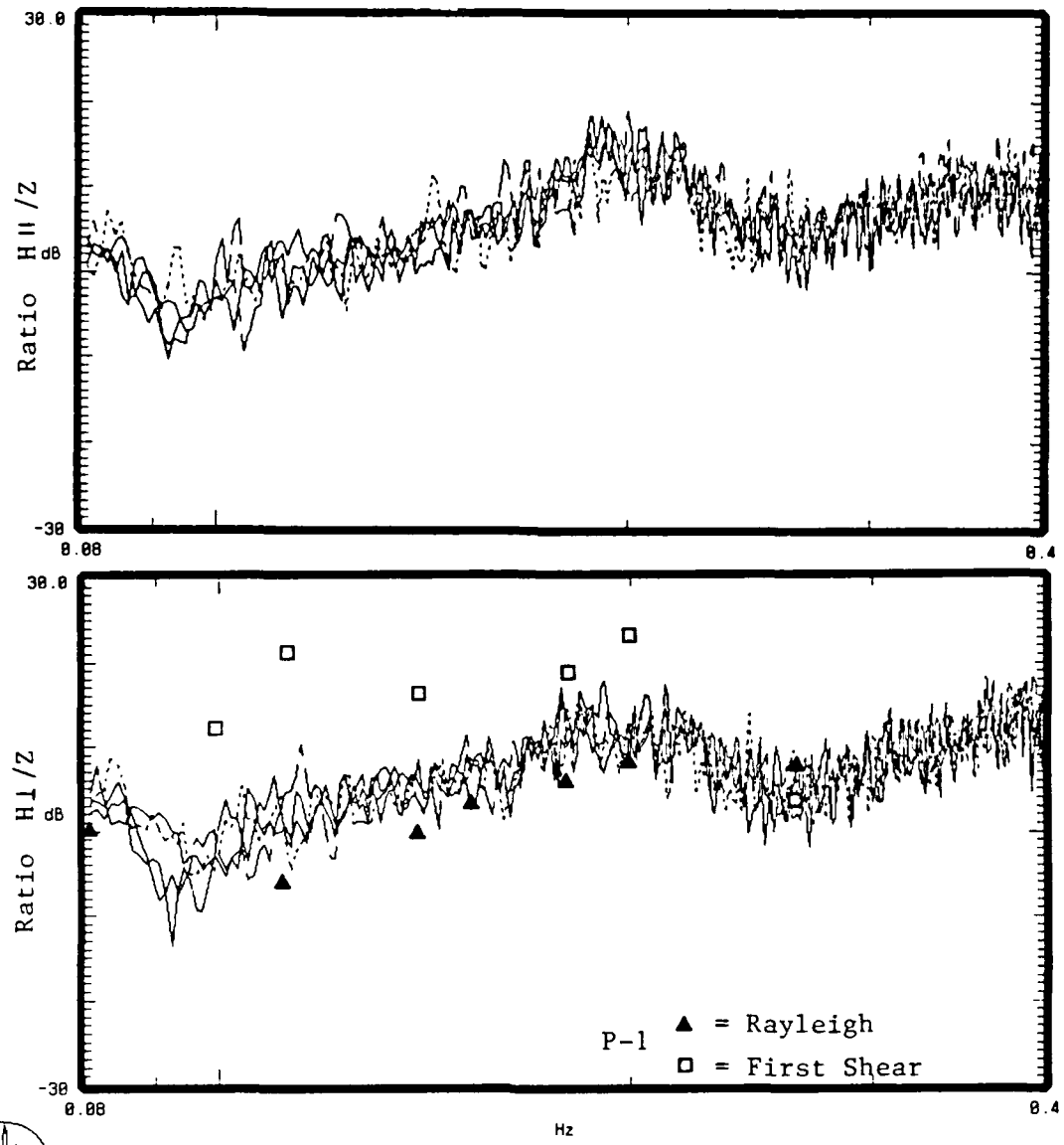

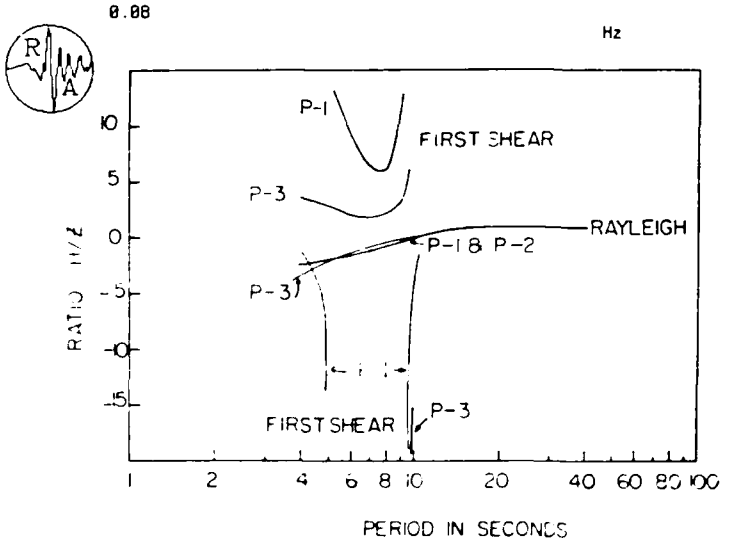

Layer Thickness, km	Compressional Velocity, km/sec	Shear Velocity, km/sec	Density, g/cc
	Model P-1		
3.800	1.51	0.00	1.03
0.010	1.51	0.15	1.65
0.100	1.60	0.19	1.70
0.100	1.71	0.37	1.79
0.100	1.80	0.53	1.86
0.200	1.90	0.70	1.90
0.500	2.20	1.10	2.05
1.400	4.70	2.70	2.54
4.600	6.90	3.98	2.90
∞	8.20	4.56	3.40

Figure 8. Horizontal-vertical spectral ratios for same time periods as Figure 5. Theoretical curves and points are from Latham and Nowroozi (1968); positive ratio indicates retrograde motion and negative ratio indicates prograde motion.

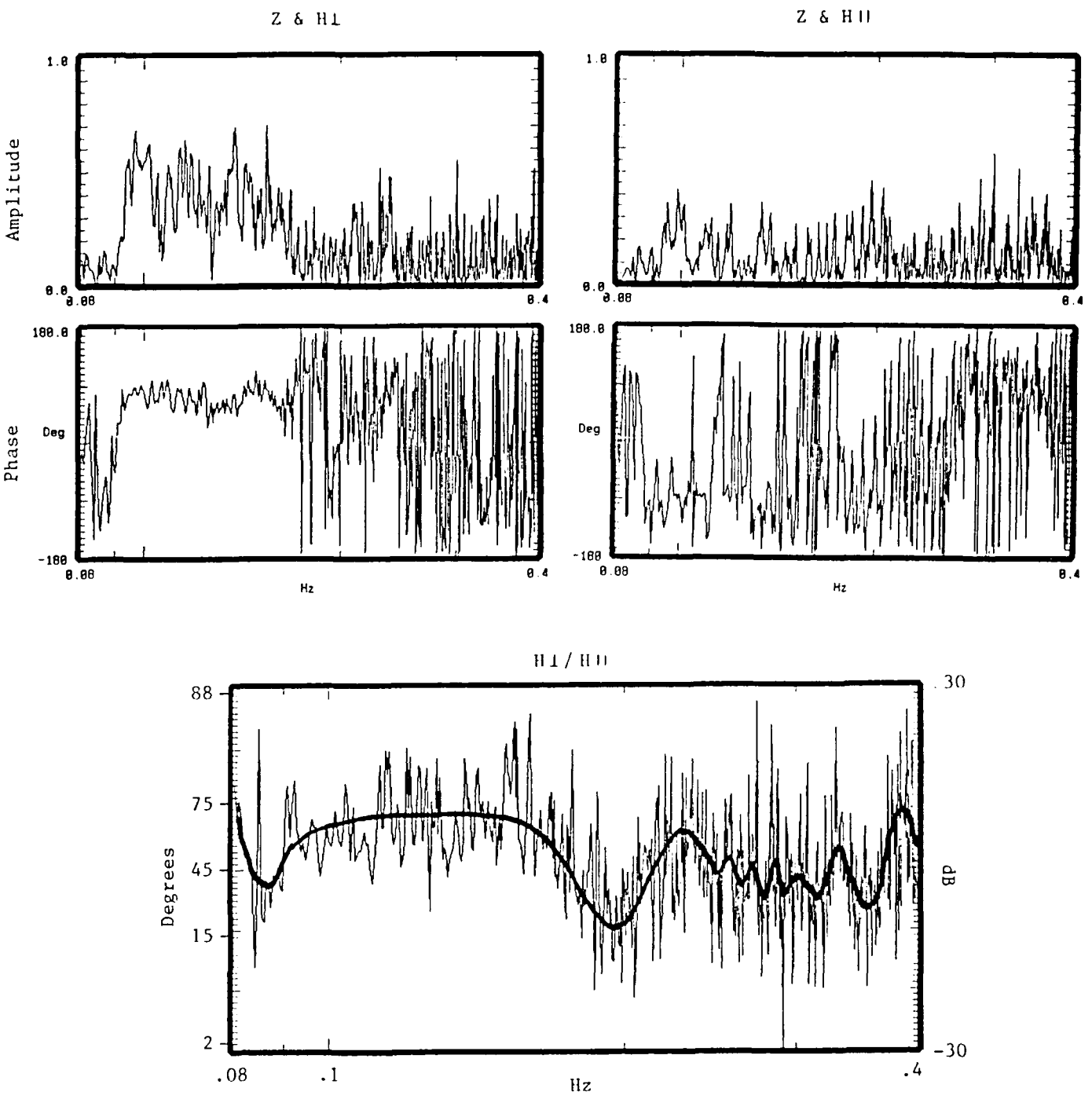

Figure 9. Coherency between vertical and horizontal motion (13-1600 UT, 12/7) and ratio of the two vertical to horizontal transfer functions. Assuming prograde Rayleigh motion, stable + or − $\pi/2$ phase identifies the proper quadrant of approach and $\tan^{-1}(H\perp/H\parallel)$ gives the angle from H||.

Unclassified

SECURITY CLASSIFICATION OF THIS PAGE

REPORT DOCUMENTATION PAGE

1a. REPORT SECURITY CLASSIFICATION Unclassified	1b. RESTRICTIVE MARKINGS
2a. SECURITY CLASSIFICATION AUTHORITY	3. DISTRIBUTION/AVAILABILITY OF REPORT Unlimited
2b. DECLASSIFICATION/DOWNGRADING SCHEDULE	
4. PERFORMING ORGANIZATION REPORT NUMBER(S)	5. MONITORING ORGANIZATION REPORT NUMBER(S)
6a. NAME OF PERFORMING ORGANIZATION Rondout Associates, Incorporated 6b. OFFICE SYMBOL (If applicable)	7a. NAME OF MONITORING ORGANIZATION Office of Naval Research
6c. ADDRESS (City, State and ZIP Code) P.O. Box 224 Stone Ridge, NY 12484	7b. ADDRESS (City, State and ZIP Code) 800 N. Quincy Street Arlington, VA 22217-5000
8a. NAME OF FUNDING/SPONSORING ORGANIZATION 8b. OFFICE SYMBOL (If applicable)	9. PROCUREMENT INSTRUMENT IDENTIFICATION NUMBER Contract No. N00014-86-C-0570
8c. ADDRESS (City, State and ZIP Code)	10. SOURCE OF FUNDING NOS. PROGRAM ELEMENT NO. / PROJECT NO. 425p001---01 / TASK NO. / WORK UNIT NO.
11. TITLE (Include Security Classification) ULF/VLF Ocean Bottom Seismo-Acoustics (U)	
12. PERSONAL AUTHOR(S) George H. Sutton	
13a. TYPE OF REPORT Final 13b. TIME COVERED FROM 1 July 86 TO 1 Jan 90	14. DATE OF REPORT (Yr., Mo., Day) 27 February 1990 15. PAGE COUNT 29
16. SUPPLEMENTARY NOTATION	

17. COSATI CODES		
FIELD	GROUP	SUB. GR.

18. SUBJECT TERMS (Continue on reverse if necessary and identify by block number)
seismo-acoustic noise, ultra low & very low frequency noise, ocean bottom microseisms, ocean bottom noise, ocean noise sources, origin of ocean seismo-acoustic noise, wind, waves & microseisms, ULF/VLF seismo-acoustic noise in the ocean

19. ABSTRACT (Continue on reverse if necessary and identify by block number)

The original research under this contract was directed toward comparison of ocean bottom seismometer and hydrophone data with ocean sub-bottom seismometer data and with appropriate synthetics to determine the effect of sub-bottom structure on the signals received; expected propagation loss; predominant modes of propagation; instrument signal distortion and excess noise; expected spacial coherence; and expected improvement from polarization and array processing. During the first and subsequent years of the contract, research emphasis was re-directed toward analysis and interpretation of data from the Columbia-Point Arena ocean bottom seismic station (OBSS) emphasizing the objectives of the ONR Accelerated Research Initiative in ULF/VLF Ocean Seismo-Acoustics.

The most extensive existing set of ocean bottom data on ULF/VLF seismic background noise and signals was obtained from OBSS, which operated for over six years (1966-1972)

20. DISTRIBUTION/AVAILABILITY OF ABSTRACT UNCLASSIFIED/UNLIMITED ☒ SAME AS RPT. ☐ DTIC USERS ☐	21. ABSTRACT SECURITY CLASSIFICATION Unclassified
22a. NAME OF RESPONSIBLE INDIVIDUAL George H. Sutton	22b TELEPHONE NUMBER (Include Area Code) (914) 687-9150 22c OFFICE SYMBOL

DD FORM 1473, 83 APR EDITION OF 1 JAN 73 IS OBSOLETE.

Unclassified

SECURITY CLASSIFICATION OF THIS PAGE

about 200 km west of San Francisco at a depth of 3900 m. The OBSS included a Lamont long-period (LP) triaxial seismometer (15 sec natural period, originally developed for lunar use); three-component short-period (SP) system (1 sec natural period); long-period (crystal) hydrophone; short-period (coil-magnet) hydrophone; ultralong-period (Vibratron) pressure transducer; thermometer; current amplitude sensor; and a current direction sensor. It was connected to shore via cable and LP and SP components were recorded separately on FM tape as well as on seismograph drum recorders. During this research, original FM tapes from the OBSS long- and short-period (LP/SP) hydrophones and LP and SP three-component seismometers were digitized to obtain ULF/VLF spectra and covariances during quiet and noisy times and during passage of vessels and earthquake wavetrains. These were compared with available source information on sea/swell condition, tidal currents, earthquakes, and shipping. Analyses were conducted in the frequency band .002 to 5 Hz.

Coherent energy peaks near 0.14, and 0.06 Hz suggest fundamental mode Rayleigh wave motion propagating shoreward. Coherent energy near .30 Hz appears to be variable. Pressure variations near 0.01 Hz and lower frequency correlate with wave heights along the California coast and appear to produce forced deformation of the bottom. Two intense NE Pacific storms with hurricane force winds occurred during one two week time period. Time variations of spectra and of amplitude and phase coherencies of the four-component OBSS data were related to the storm histories and to local weather/wave conditions and used to identify motion (seismic wave) types and directions of propagation.